

Experimental and Numerical Stability Analysis of Cable in Conduit Superconductor for the ITER Project

by

Kevin Stanley McFall

B.S., Mechanical Engineering (1995)
Virginia Polytechnic Institute and State University

Submitted to the Department of Mechanical Engineering
in Partial Fulfillment of the Requirements for the Degree of

MASTER OF SCIENCE IN MECHANICAL ENGINEERING

at the

MASSACHUSETTS INSTITUTE OF TECHNOLOGY

May 1997

© Massachusetts Institute of Technology 1997. All rights reserved.

The author hereby grants to MIT permission to reproduce and
to distribute copies of this thesis document in whole or in part.

Signature of Author _____
Department of Mechanical Engineering
May 27, 1997

Certified by _____
Yukikazu Iwasa
Thesis Supervisor

Accepted by _____
Ain A. Sonin
Chairman, Departmental Graduate Committee

MASSACHUSETTS INSTITUTE
OF TECHNOLOGY

JUL 21 1997 Eng.

LIBRARIES

Experimental and Numerical Stability Analysis of Cable in Conduit Superconductor for the ITER Project

by

Kevin Stanley McFall

Submitted to the Department of Mechanical Engineering
in May 1997, in partial fulfillment of the
requirements for the Degree of
Master of Science in Mechanical Engineering
at the Massachusetts Institute of Technology

Abstract:

The pursuit of a commercial plasma fusion reactor has met with many technological difficulties not least of which is producing reliable high magnetic fields. The large scale of the magnet systems involved presents difficulties and high cost for extensive experimental investigation. For this reason an accurate simulation of the behavior of the conductor can be of great service. Of the properties of the magnetic systems, one of the most important is its resilience to thermal disturbances in maintaining the superconducting state. To study this stability the simulation code POCHI has been developed at the Japan Atomic Energy Research Institute. While this code has proven useful in predicting behavior of NbTi conductors its application to Nb₃Sn has not been as successful. As Nb₃Sn is the material to be used for the central solenoid coil, it is desired that POCHI be improved to extend its applicability to this material as well. Presented here is a description of two versions of POCHI and comparison of POCHI results with experimental data. Both version of the simulation predict higher stability margins than from experimental data although the shape of the curves are all rather similar. Results from POCHI v4 do not indicate a significant improvement over version 3. Experimentally, it was not possible to determine the precise limiting current for this conductor; suggesting it may be over 5000A.

Thesis Supervisor: Dr. Yukikazu Iwasa

Title: Research Professor, Francis Bitter Magnet Laboratory, and
Senior Lecturer, Department of Mechanical Engineering, MIT

Acknowledgment:

First of all I would like to thank Joe Minervini and the Plasma Science and Fusion Center of MIT for finding the resources to fund my research assistantship. Without this support none of my work would have been possible. Also of great importance to me is all the help provided by Paul Berger and the entire MIT Japan Program. I truly appreciate the countless hours spent to organize seminars and retreats which made my transition to Japanese life as smooth as possible. My thanks go out to Hiroshi Tsuji for welcoming me into the Superconducting Magnet Laboratory and helping make a contribution to ITER project. Another name which certainly could not go unspoken is Norikiyo Koizumi whose patience and expertise were always there, whether I was working together with him in Japan or continuing after returning to MIT. And finally there is Yukikazu Iwasa who played a very important role from start to finish in my time at MIT. Not only has he introduced me to the field of superconducting magnets, but made possible all the wonderful experiences I've had in the past two years both at MIT and in Japan.

Table of Contents

1. Introduction

2. Improvement to POCHI

2.1 POCHI Basic Model

2.2 Implementation of Conduction in the Boundary Layer

2.3 Nonuniform Mesh Transformation

3. Experimental Techniques and Procedures

3.1 Test Coil Description and Experiment Preparation

3.2 Experiment Operating Conditions

3.3 Discussion of Inductive Heater

4. Comparison Between Experiment and POCHI

4.1 Experiment 1

4.2 Experiment 2

4.3 Effects of r on Simulation Results

5. Conclusion

References

Appendix - Code for POCHI 4 Implementation

1. Introduction

Much work is currently underway to overcome the technological obstacles involved with the International Thermonuclear Experimental Reactor (ITER). Among these challenges is producing a high magnetic field stable against thermal disturbances. ITER is to use superconductors of the cable in conduit conductor (CICC) type cooled by forced flow supercritical helium. There has been much research in the area of stability of CICC's and as a result it has become apparent that the magnets should be designed to operate in the so-called well-cooled regime¹. Well-cooled operation offers the best possibility of maintaining cryostability in the face of disturbances to the conductor. In order to ensure well-cooled operation, determination of the limiting current for the conductor in question is of great importance. The most reliable method for locating the transition from well to poorly-cooled regimes is experimental. However, ITER is of such a large scale that extensive testing of the actual conductor is impractical. For this reason a reliable computer simulation code is indispensable in predicting the behavior of superconductors. Much work has been done at the Superconducting Magnet Laboratory of the Japan Atomic Energy Research Institute (JAERI) to develop a code suitable for predicting the performance of CICC's against thermal disturbances. This simulation code, named POCHI, was developed using an implicit time-dependent finite difference algorithm developed by Norikiyo Koizumi². POCHI requires further refinement to make it useful for the design of ITER's magnets.

Of the several conductor types possible for constructing large superconducting magnets, ITER has chosen CICC's. Conductors of this type have small, multifilamentary strands of superconductor encased in a leak-tight conduit. The strands do not occupy the entire conduit cross section and the remaining area is occupied by supercritical helium that is forced through the conduit to cool the strands. One of the main strengths of CICC's is the mechanical support offered by the conduit to withstand large Lorentz forces in the magnet winding.

Stability margin is of great importance to the magnet designer as it quantifies the conductor's stability against a thermal energy disturbance. Stability margin, generally given in units of mJ/cm^3 , is defined as the minimum energy density (based on the current carrying conductor volume)

which will force the conductor from the superconducting to normal state. In the past as reported by Koizumi³, for similar conditions as investigated in this report but with the NbTi conductor, POCHI v3 agreed with experiment for all stability margin data points in the region of the limiting current within 20%. Only recently has simulation of stability of Nb₃Sn conductors by POCHI been investigated. Unfortunately the preliminary results have not shown as good an agreement for this conductor as for NbTi, most likely due to high transport currents and background magnetic fields associated with Nb₃Sn. However it is believed that improvement in the modeling of the strand-to-coolant heat transfer will enable POCHI to predict accurate results for Nb₃Sn as well. By replacing the analytically derived heat transfer coefficient, which among other things does not account for the effect of a changing boundary layer on the heat transfer, with direct solution of the temperature profile within the coolant, we expect to upgrade POCHI. Presented in this paper are the steps towards this goal.

In order to test the effectiveness of POCHI v4, two experiments were conducted. As POCHI is to be applied to ITER, these experiments used the conductor from the ITER central solenoid (CS) coil. The full sized CS coil is designed for an operating transport current of 40 kA and a peak field of 13T and with a coolant flow rate of approximately 15 g/s. Due to the obvious difficulties associated with testing the full size CICC coil, a 1/24 scaled down sample conductor was manufactured. This conductor is a 48-strand Nb₃Sn CICC (appropriate conductor parameters are listed in table 1). The first experiment was performed to obtain data to compare with results from POCHI v3 and v4. The purpose of the second experiment was to determine the limiting current and compare it with that predicted by POCHI.

2. Improvement to POCHI

2.1 POCHI Basic Model

As the turbulent boundary layer under typical operating conditions in the conductor is smaller than the interstrand distance, POCHI uses a one dimensional tube flow model in the simulation of mass and heat flow; the conductor's hydraulic diameter is a characteristic length. Equation 1 expresses the governing equation for the coolant³.

$$\frac{\partial u}{\partial t} + \frac{\partial F}{\partial x} + G = 0 \quad (1)$$

$$\text{where } u = \begin{bmatrix} \rho \\ \dot{m} \\ E \end{bmatrix} \quad F = \begin{bmatrix} \dot{m} \\ \frac{\dot{m}^2}{\rho} + p \\ \dot{m}(E + p) \end{bmatrix} \quad G = \begin{bmatrix} 0 \\ \frac{4\sigma}{d_h} \\ -\frac{P_{st}q_{st} + P_{con}q_{con}}{A_{He}} \end{bmatrix}$$

With coolant density ρ , flow rate \dot{m} , internal energy E , pressure p , friction stress due to coolant flow σ , hydraulic diameter d_h , strand perimeter P_{st} , heat transferred from the strands to the coolant q_{st} , conduit perimeter P_{con} , heat transferred from the conduit to the coolant q_{con} , and coolant cross sectional area A_{He} . Treatment of the coolant is identical in POCHI v3 and v4. The improvement lies in the heat conduction in the strands, as expressed below.

$$\gamma_{st} \frac{\partial T_{st}}{\partial t} - \lambda_{st} \frac{\partial}{\partial x} \left(\frac{\partial T_{st}}{\partial x} \right) - q_{st} + Q_{st} = 0 \quad (2)$$

Where γ_{st} is volumetric heat capacity, T_{st} is temperature, λ_{st} is thermal conductivity of the strand, and Q_{st} is joule heating generated within the conductor. In the POCHI v3, q_{st} is calculated using an analytical heat transfer coefficient and the temperature difference between the strand and bath helium temperatures. The proposed improvement is to calculate explicitly the temperature profile in the coolant helium. This replaces the one dimensional temperature scheme in POCHI v3 with the two dimensional mesh as shown in figure 1. The x direction remains essentially unchanged in the two versions, calculating the temperature profile within the strands in the axial direction with equation 2. The difference between the two version lies in the definition of q_{st} . Equation 3a

defines q_{st} for POCHI v3 and equation 3b for POCHI v4.

$$q_{st} = h(T_{st} - T_{bath}) \quad (3a)$$

$$q_{st} = h_k(T_{st} - T_{He}|_{y=0}) \quad (3b)$$

Where T_{bath} is the helium bath temperature at the centerline of the hydraulic diameter and T_{He} is the coolant temperature which is assumed y -dependent at a given point in x . The heat transfer coefficient h is derived by Carlslow and Jaeger⁴ who do not account for variation in boundary layer caused by unsteady coolant flow. The Kapitza conductance⁵, h_k in units of W/m²K and defined in equation 4, is used in POCHI v4.

$$h_k = \frac{200 \left[T_{st}^4 - (T_{He}|_{y=0})^4 \right]}{T_{st} - T_{He}|_{y=0}} \quad (4)$$

The y axis, which is the strand radial direction, begins at the strand surface ($y=0$) and extends out to the boundary layer. This is the major addition comprising version 4 in which the temperature profile in the coolant, $T_{He}(y, x_0)$, is calculated. In order to minimize the extra CPU time added by calculation of the helium temperature mesh, this model assumes heat conduction in the helium to be directed only in the y -axis.

2.2 Implementation of conduction in the boundary layer

The main weakness of POCHI is its the heat transfer from the strands to the coolant. This topic has received much attention in the past by Koizumi². Even after several improvements, a heat-transfer coefficient derived mathematically rather than the temperature profile in the coolant derived from the heat equation was used for this heat transfer. The proposed method to evaluate q_{st} in POCHI v4 is to instead use the Kapitza conductance, h_k , and the temperature difference between the strand and the first node in a temperature mesh for the coolant as in equation 3b. The coolant temperature mesh is solved from equation 5 below.

$$\gamma_{He} \frac{\partial T_{He}}{\partial t} - \lambda_{He} \frac{\partial^2 T_{He}}{\partial y^2} = 0 \quad (5)$$

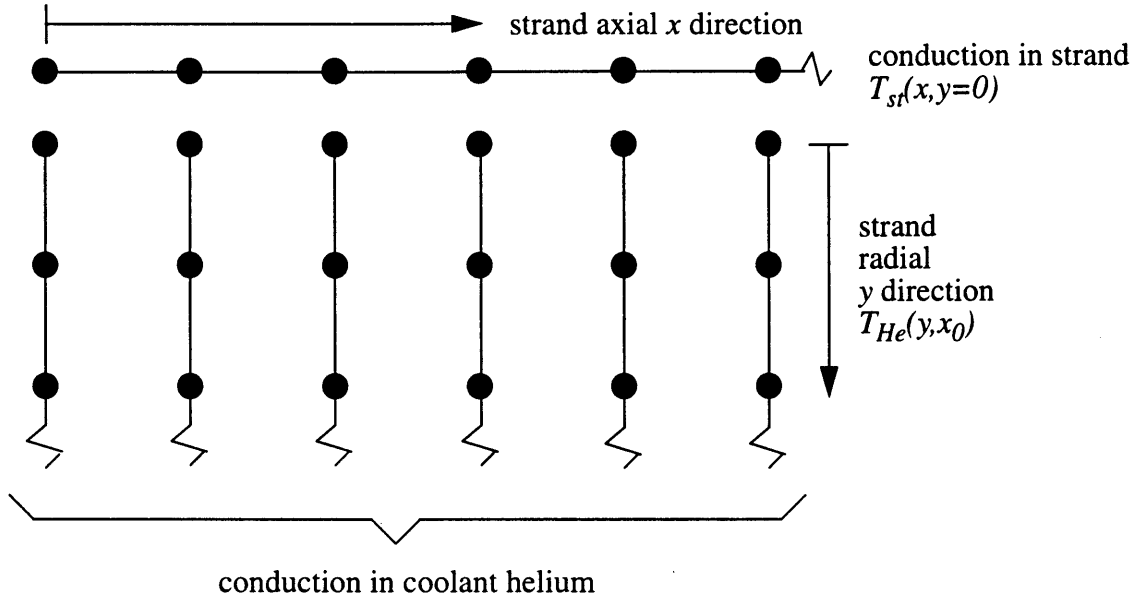


Figure 1: Diagram of x and y meshes for numerical grid in POCHI v4.
Each dot represents a node within the boundary layer.

The boundary condition at the strand surface equates the Kapitza heat transfer equation 3b to equation 5. The other boundary simply equates coolant temperature with the helium bath temperature.

$$h_k(T_{st} - T_{He}|_{y=0}) = \lambda_{He} \frac{\partial T_{He}}{\partial y} \Big|_{y=0} \quad (6a)$$

$$T_{He}|_{y=0} = T_{bath} \quad (6b)$$

Coolant mass flow rate \dot{m} is calculated by POCHI according to equation 1 and can vary significantly in the heated region and thus the boundary layer δ must be defined for both laminar and turbulent flows.

$$\delta = \begin{cases} \frac{d_h}{0.023 Re^{0.8} Pr^{0.4}} & (\text{turbulent}) \\ \frac{d_h}{2} & (\text{laminar}) \end{cases} \quad (7)$$

With Reynolds number Re , and Prantl number Pr . In the turbulent case, the heat transfer is dominated by the small thermal boundary layer while laminar flow has no definitive boundary layer

and thus temperature gradients exist all the way to the centerline of the modeled tube of diameter d_h . The boundary layer for the turbulent case is approximated with an empirical relation for the steady state heat transfer coefficient⁶.

2.3 Non-uniform mesh transformation

Heat transfer is important near the strand surface and it is thus desirable to have a fine mesh in the y direction to obtain accurate results. However, with lower temperature gradients farther from the strand surface, such a fine mesh would unnecessarily increase CPU time. For this reason the non-uniform mesh resulting from a transformation from the physical y coordinate to the general coordinate ξ as per Thompson and Mastin⁷ is used. This transformation can be expressed as in equation 8 for arbitrary variable Z .

$$\frac{\partial Z}{\partial t} = \frac{\partial Z}{\partial \tau} - \frac{y_\tau \partial Z}{y_\xi \partial \xi} \quad (8a)$$

$$\frac{\partial Z}{\partial y} = \frac{1}{y_\xi} \frac{\partial Z}{\partial \xi} \quad (8b)$$

$$\frac{\partial^2 Z}{\partial y^2} = \frac{1}{y_\xi^2} \left(\frac{\partial^2 Z}{\partial \xi^2} - \frac{y_{\xi\xi} \partial Z}{y_\xi \partial \xi} \right) \quad (8c)$$

$$\text{where} \quad y_\tau = \frac{\partial y}{\partial \tau} \quad y_\xi = \frac{\partial y}{\partial \xi} \quad y_{\xi\xi} = \frac{\partial^2 y}{\partial \xi^2}$$

For this application there will be no transformation in time so τ may be replaced with t . With this transformation the governing equation for the heat transfer in the coolant becomes (note *He* subscript has been omitted for clarity):

$$\gamma \left(\frac{\partial T}{\partial t} - \frac{y_t \partial T}{y_\xi \partial \xi} \right) = \frac{\lambda}{y_\xi^2} \left(\frac{\partial^2 T}{\partial \xi^2} - \frac{y_{\xi\xi} \partial T}{y_\xi \partial \xi} \right) \quad (9)$$

In discrete form with first order accuracy in time and second order in space, equation 9 becomes:

$$\gamma \left[\frac{T_j^n - T_j^{n-1}}{\Delta t} - \frac{y_t}{2y_\xi \Delta \xi} (T_{j+1}^n - T_{j-1}^n) \right] = \frac{\lambda}{y_\xi^2 \Delta \xi} \left[\frac{T_{j+1}^n - 2T_j^n + T_{j-1}^n}{\Delta \xi} - \frac{y_{\xi\xi}}{2y_\xi} (T_{j+1}^n - T_{j-1}^n) \right] \quad (10)$$

Where time is superscripted as n and space subscripted as j . POCHI v4 implements this equation to solve for the temperature profile within the coolant helium and use the Kapitza conductance and coolant temperature gradient at the strand surface to solve for the heat transfer to the coolant. POCHI v4 thus eliminates the need for the analytically derived heat transfer coefficient used in POCHI v3. It is important to note that POCHI v4 upgrades only the conduction from the strands and that from the conduit remains calculated as in the POCHI v3.

3. Experimental Techniques and Procedures

3.1 Test Coil Description and Experiment Preparation

Stability testing was performed on the 1/24 size central solenoid conductor to obtain experimental data to compare with POCHI. The procedure, sample, and equipment were identical for the two experiments. The relevant parameters of the conductor and test coil are listed in Table 1.

Figure 2 shows a schematic of the liquid helium temperature region of the experimental apparatus. The conductor is wound into a test coil of 10 turns with a total length of 7.1 m and an inductive heater attached to a 6.6 cm length of the test coil. Heat is generated in the conduit and the non-superconducting section of the strands by eddy currents induced by a 5 or 40 ms long 1 kHz sinusoidally varying magnetic field pulse generated by the heater. The test coil was inserted into

Table 1: Parameters for Conductor and Test Coil Used in Both Experiments

Conductor Description		
Strand	Number of strands	48
	Material	Nb ₃ Sn
	Diameter	0.92 mm
	Copper/non-copper ratio	1.58
	Twist pitch	20 mm
	Cr plating thickness	2 μm
Conduit	Material	Ti
	OD	9.84 mm
	ID	8.05 mm
	Void fraction	35.4%
Test coil	OD	209.7 mm
	ID	190.0 mm
	Turns	10
	Total conductor length in the coil	7.1 m

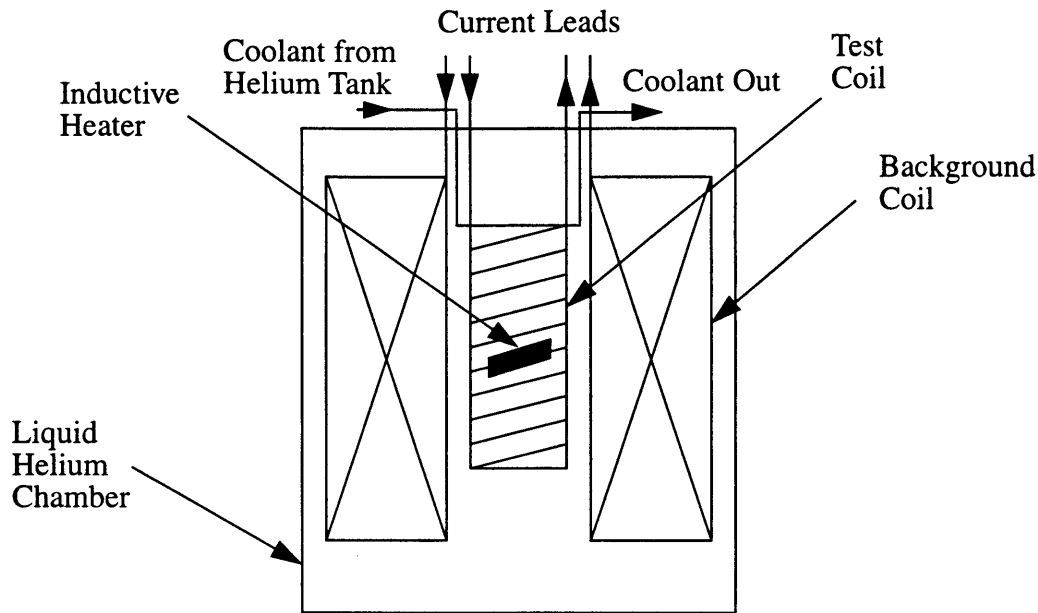


Figure 2: Schematic of experimental apparatus showing liquid helium temperature section.

the superconducting background coil. The background magnet can expose a maximum field of 13T at the site of the inductive heater. During operation the helium vessel is filled with liquid helium to keep the background magnet at 4.2K and to cool the current leads for both the background magnet and test coil. The cooldown procedure consisted of first filling both chambers with liquid nitrogen and then pumping the inner chamber to reduce the saturation temperature of the nitrogen towards 64K. Nitrogen was then pumped out and the inner chamber filled with liquid helium. After the background magnet and test coil were cooled down to 4.2 K and thus superconducting, they could be charged. The current of the background magnet was ramped up to an appropriate level for the background field desired; 1074 A for 11T, 1172 A for 12T, and 1271A for 13T. Once the background field level was achieved, the test coil was energized by ramping up its current to the level for the data point to be measured. Stability margin was determined by successively increasing the level of heating pulse until a quench was observed. The stability margin thus falls between that corresponding to the highest recovery point and that corresponding to the quench; the margin is the arithmetic average of these two values. An energy increment was typically 200 mJ/cm^3 . Test coil current was dropped to zero for each quench event and the measurement was resumed once the test coil returned to steady state.

3.2 Experiment Operating Conditions

Coolant is delivered to the test coil at 4.2K, 6 atm., and 0.2 g/s mass flow rate maintained during the entire experiment duration. In the first experiment the inductive heater was excited for 5 ms with a background field of 13T, a level that caused two quenches of the magnet itself. Consequently the experiment was completed with a background field of 12T. For the second experiment a heating pulse of 40 ms was used and the background magnet was set at 11T.

3.3 Discussion of inductive heater

During the mid 1980's, calibration of the inductive heater for this conductor in a background field of 13T was performed. The method for this calibration was identical as that performed by Ito⁸ in a recent experiment on a NbTi conductor. The heater delivers a sinusoidal wave pulse with a frequency of 1 kHz. The total energy delivered to the system by the heater, E_{tot} , can be expressed in terms of E_{con} , total heat delivered to the conduit, E_{st} , total heat delivered to the strands, and E_{heat} , the total energy dissipated in the inductive heater.

$$E_{tot} = E_{con} + E_{st} + E_{heat} \quad (11)$$

Each energy may be expressed in the form given below:

$$E = C \int_0^{\tau} I^2(t) dt \quad (12)$$

where τ is the heating duration and $I(t)$ is the current through the heater. The calibration experiment measured the amount of helium boiled off for three different conditions: 1) with the inductive heater alone (E_{heat}); 2) with the inductive heater and an empty conduit ($E_{heat} + E_{con \text{ alone}}$); 3) with the full conductor (E_{tot}). For each condition C in equation 12 could be determined. As the energy released by the heater E_{heat} is independent of heating initiated in the strands and conduit, both E_{heat} and E_{tot} can be determined experimentally. Unfortunately, because $E_{con \text{ alone}} < E_{con}$ due to the coupling of the eddy currents between the conduit and strands, E_{st} cannot be solved for by simple subtraction. Ito found, through calculations, that the coupling effect between the conduit (stainless steel) and strands was minimal and thus ignored. However the conduit material in this experiment was titanium, more conductive (perhaps by two orders of magnitude) than stainless steel. The coupling effect in this case cannot be ignored. To determine the range within

which the stability margin would fall, the simulation can be run for two cases; 1) with $E_{con}=E_{con\ alone}$; and 2) with $E_{con}=0$. Of course the true value will be closer to the first case and the $E_{con}=0$ case is simply a lower limit. Since POCHI handles heat originating from the strands and that from the conduit differently, the distribution of heat in the conduit and strands could not be exactly matched between the simulation and experimental results. A value of $E_{con\ alone}/E_{st}=2.3$ for the Nb₃Sn conductor used in the test coil was believed to be the correct calibration. Hereafter, $E_{con\ alone}/E_{st}$ is referred to as r , the heating ratio. Since POCHI v3 was run during the period of time when the correct value of r was believed to be 2.3, all of the runs for POCHI v3 used $r=2.3$. However it was later discovered that this value was not 2.3 but 3.8. This complicated comparisons between POCHI v3 and v4 as well as the experimental data. The calibration data were never formally documented by passed down through private communication at JAERI. Another source of uncertainty is that the calibration was conducted for a background field of 13T and the data were taken at 11 and 12T; r cannot be expected to be field independent although the nature of its dependence is difficult to quantify.

During the experiment, data acquisition returns $\int_0^\tau I^2 dt$, which multiplied by $(C_{tot} - C_{heat})$, produces an energy supplied to the conductor (conduit and strands). The uncertainty falls in how this energy is distributed among the conduit and strands. In order to check the calibration results, $E_{con\ alone}$ is solved for analytically as follows. Figure 3 shows a schematic arrangement for the inductive heater and conduit. The heating power density P_{con} in the conduit can be expressed in terms of the electric field E induced and the resistivity ρ_{con} of the conduit material, titanium.

$$P_{con} = E^2/\rho \quad (13)$$

Note that the value of ρ , $2 \times 10^{-8} \Omega m$ given in figure 3 is for titanium at 4.2 K and zero magnetic field. As the resistivity is relatively high (~100 times that of copper at 4.2 K in zero field), its dependence on magnetic field can be assumed negligible; this value is used even for fields of 11-13 T. Integrating equation 13 over the heating duration τ yields energy density $E_{con\ alone}$.

$$E_{con\ alone} = \int_0^\tau P_{con} dt = \int_0^\tau (E^2/\rho) dt \quad (14)$$

$$\begin{aligned} \delta &= 8.95 \times 10^{-4} \text{ m} \\ \bar{R} &= 4.473 \times 10^{-3} \text{ m average radius} \\ 2b &= 6.6 \times 10^{-2} \text{ m} \\ 2a_1 &= 1.172 \times 10^{-2} \text{ m} \\ 2a_2 &= 2.276 \times 10^{-2} \text{ m} \\ \omega &= 2\pi \times 10^3 \text{ rad/s} \\ \tau &= 5 \text{ or } 40 \text{ ms} \\ \rho &= 2 \times 10^{-8} \Omega \text{ m} \\ N &= 160 \text{ turns in inductive heater} \end{aligned}$$

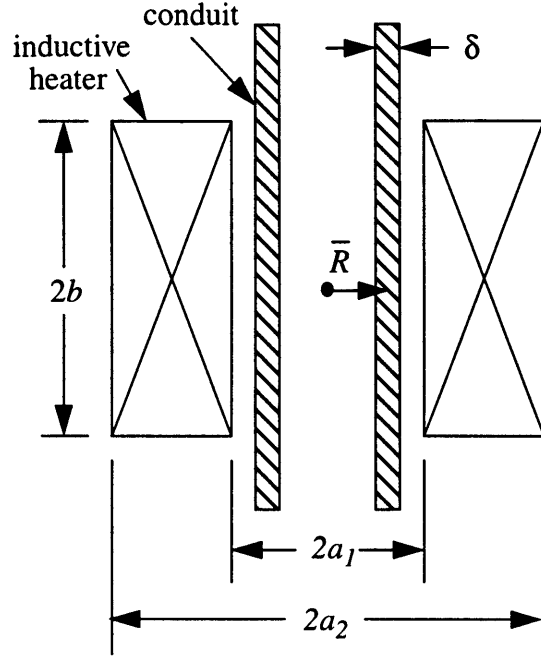


Figure 3: Schematic of and parameters for inductive heater and conduit (not to scale)

For “low” frequencies the electric field produced in the conduit by dB/dt from the inductive heater can be assumed decoupled:

$$\oint_C \vec{E} \cdot d\vec{s} = \frac{\partial}{\partial t} \oint_S \vec{B} \cdot d\vec{A} \quad (15a)$$

$$2\pi\bar{R}E = -\pi\bar{R}^2 \frac{dB}{dt} \quad (15b)$$

where \bar{R} , as shown in figure 3, is the average radius of the conduit. Equation 15b is valid because $\delta \ll \bar{R}$ for this conduit. The “low” frequency approximation is valid as long as the excitation frequency is lower than skin depth frequency⁸, f_{sk} .

$$f_{sk} = \frac{\rho}{\pi\mu_0\bar{R}\delta} \quad (16)$$

which with the parameter values in figure 3 inserted into equation 16 becomes 1.3 kHz. As the excitation frequency is 1kHz the “low” frequency approximation is valid. Assuming the inductive heater to be a straight solenoidal, the dependence of the $B(t)$ on heater transport current $I(t)$ can be expressed as:

$$B(t) = DI(t) \quad (17)$$

where D is a field constant. The software SOLDESIGN was used to compute D , $D = 1.2515 \times 10^{-3}$ T/A at \bar{R} . Differentiating equation 17 yields:

$$\frac{dB}{dt} = D \frac{dI(t)}{dt} \quad (18)$$

By combining equations 14, 15b, and 18, we have an expression for the energy dissipation density $e_{con\ alone}$ in the conduit.

$$e_{conalone} = \frac{(\bar{R}D)^2}{4\rho} \int_0^\tau \left[\frac{dI(t)}{dt} \right]^2 dt \quad (19)$$

For $I(t) = I_0 \cos \omega t$, equation 19 becomes:

$$e_{conalone} = \frac{(\bar{R}D\omega I_0)^2 \tau}{8\rho} \quad (20a)$$

$$= 3.093 \times 10^2 I_0^2 [J/(m^3 A^2)] \quad (20b)$$

For 24 data points taken during experiment 2, the average value of I_0 was 42.2 A and thus from equation 20b $e_{conalone} = 550$ mJ/cm³. Also averaged over the twenty four data points is the experimentally determined energy density dissipated in the conductor in equation 21.

$$e_{tot} - e_{heat} = e_{con} + e_{st} = 1054 \text{ mJ/cm}^3 \quad (21)$$

Again approximating $e_{con} \approx e_{conalone}$ and combining equations 20b and 21 we obtain a value of $r=1.1$, which disagrees with the calibration value of 3.8 which is believed to be the correct value from calibration. The main source of uncertainty in the calculation presented here is the value of $\rho = 2 \times 10^{-8}$ Ωm for titanium at 4.2 K given for zero magnetic field.

4. Comparison Between Experiment and POCHI

4.1 Experiment 1

The first experiment was conducted to obtain data to test the two versions of POCHI, POCHI v3 and POCHI v4. Graphed together in figure 4 are the results from the first experiment and the simulation results from POCHI v3 and v4. At the time POCHI v3 was run, r was believed to be 2.3 and so the results from figure 1 are deduced with $r=2.3$ and a background field of 12T. The data from POCHI v3 resembles the shape of the experimental data quite well but overshoots by a nearly constant factor of two. POCHI v3 and v4 results are rather close although version 4 exhibits a somewhat higher slope. These two curves do not indicate a well-defined transition from well

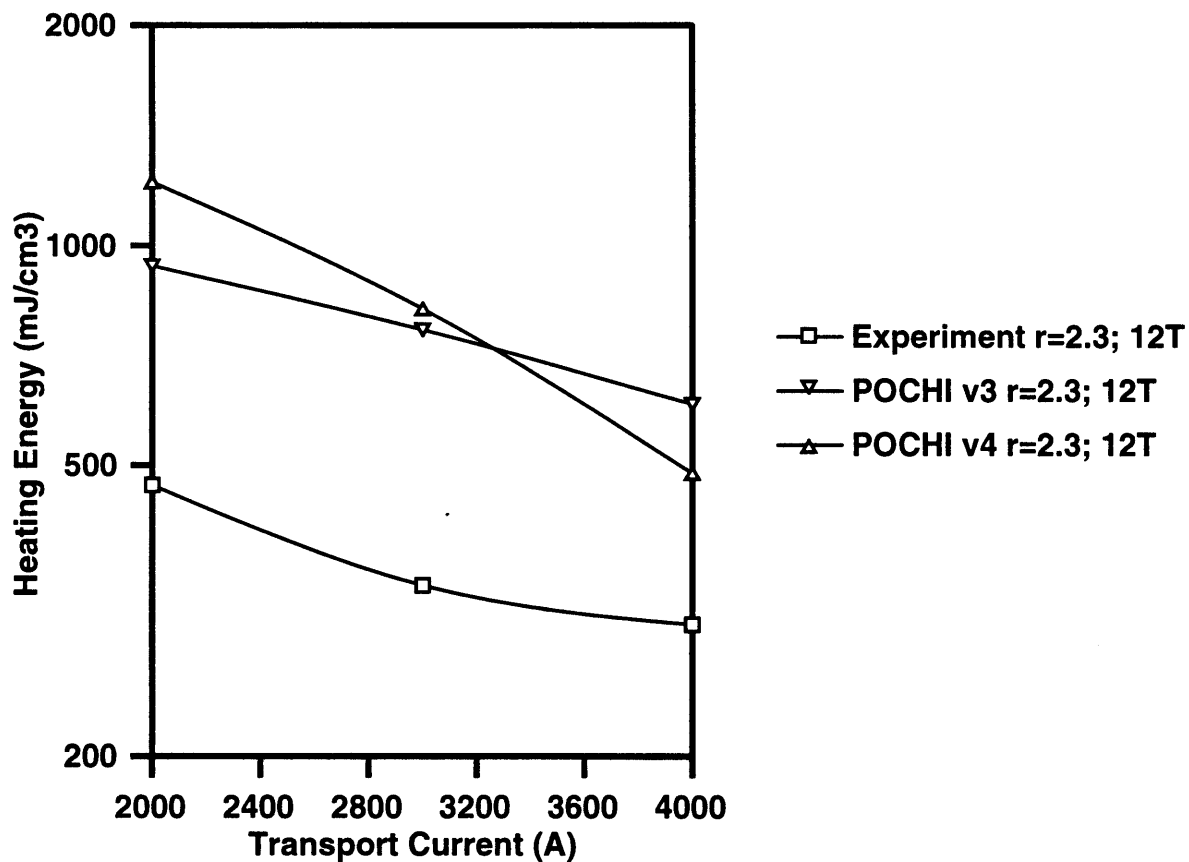


Figure 4: Stability margin vs. transport current from experiment 1 and two versions of POCHI.

All data are at 12T background field, 5 ms heating pulse, and $r=2.3$

to poorly-cooled operation which occurs at the limiting current¹. With only 3 data points over a range of 2000 A, however, detecting a limiting is difficult.

4.2 Experiment 2

The purpose of experiment 2 was to determine the limiting current for the conductor. The heating duration was increased to 40 ms as the first experiment, at 5 ms, was unable to locate the limiting current. As experiment 1 produced a rather flat stability margin/transport current profile, the heating duration for experiment 2 was extended to 40 ms since a longer heating duration would more likely cause the test coil to exhibit a more well-defined limiting current. Graphed in figure 5 are

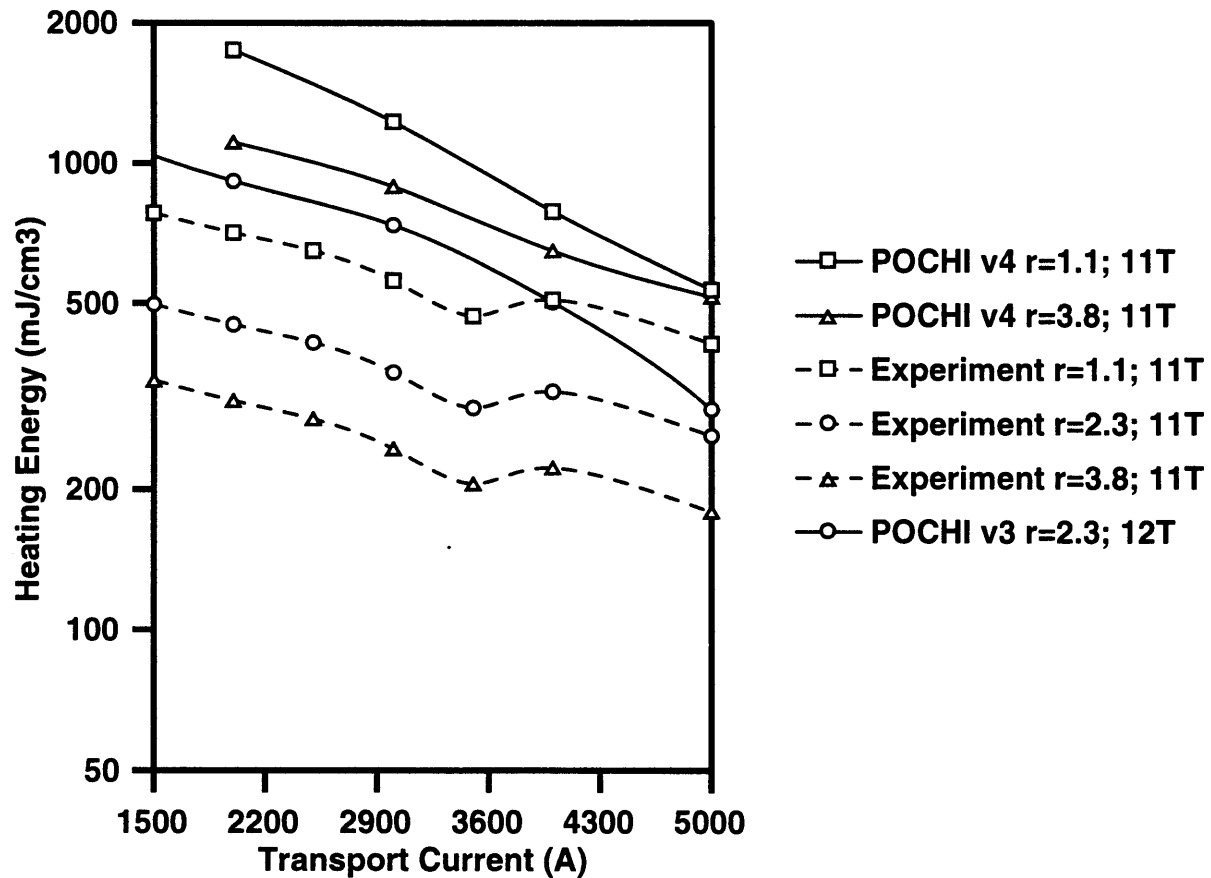


Figure 5: comparison of POCHI v3 and v4 with experiment and illustration of simulation dependence on r.

All data at 11T and 40 ms heating pulse except POCHI v3 at 12T.

the results from experiment 2 and POCHI v3 and v4. All data was calculated with a background field of 11T except for the 12T used in POCHI v3. This makes the POCHI v3 data appear lower as reducing the background field will drive the stability margin higher. POCHI v4 was not run with $r=2.3$ as version 3 was since it is known that 2.3 is not the correct calibration for r . Instead POCHI v4 was run at values of $r=1.1$ and $r=3.8$ to compare agreement between experimentally and theoretically determined values for r .

The comparison of POCHI with experiment shows that the simulation overshoots the experimental data for both versions but that in general the shapes of the curves are all fairly similar. There appears to be an aberration in the experimental data around the 3500 and 4000 A points since they do not form a smooth curve. In any case the experiment still does not show the rapid decline in stability margin associated with cooling regime transition. Even increasing the heating duration to 40 ms did not help in discovering the limiting current.

4.3 Effect of r on Simulation Results

Figure 5 above shows the results of experiment 2 and simulation (POCHI v4) for two values of r , 1.1 which is predicted by theory, and 3.8 which is now believed the correct obtained from experimental calibration. For a constant energy input to the strands, one would expect that raising the value of r would tend to drive the stability margin down since more total heat is introduced to the system while the same energy is delivered to the strands. The results from the simulation show this to be true as stability for $r=3.8$ is lower than that for $r=1.1$. Also it should be noted that the stability margin from the experiment is dependent on r as total energy was measured which must be divided between the conduit and strands as determined by the value of r . For $r=1.1$, the percentage error between POCHI v4 and experiment is 88% and that for $r=3.8$ is 225%. For the theoretically determined $r=1.1$, the simulation agrees much more closely than with the calibration value of $r=3.8$. It should be noted that since stability margin is dependent on r , it is thus dependent on the heat conduction from the conduit to the coolant which is calculated by the old technique as in POCHI v3. Perhaps better agreement can be achieved if the modification of POCHI v4 is applied to the conduit heat transfer as well.

5. Conclusion

In order to facilitate the design of large superconducting magnet systems like those involved with ITER, an accurate simulation program can be extremely effective in reducing the need for expensive experiments. The simulation code POCHI developed at JAERI has shown in the past to be quite accurate in predicting the limiting currents for NbTi based CICC. With Nb₃Sn conductors POCHI has been less successful. As this is the material of choice for most of ITER's magnets, improving POCHI is of great importance. The experiment described in this paper tested both versions in terms of their ability to predict stability margins and limiting currents for a test coil wound with a 1/24 scale model of the ITER Nb₃Sn CICC. Also presented here is the upgrade from POCHI v3 to POCHI v4, whose differences lie in the treatment of the heat transfer from strand to coolant.

Results presented seem to suggest v4 is not significantly better than v3 at predicting stability margins as measured experimentally. Although there is a serious source of uncertainty in the calibration of the inductive heater, simulation results overshoot experimental data for all values of the calibration parameter r , defined as $E_{con\ alone}/E_{st}$. The closest agreement, at an average 88% error, is between experiment 2 and POCHI v4 using a value of $r=1.1$ which is predicted by theory. Also of importance is locating the limiting current for this conductor. Neither experiment 1 nor 2 have exhibited a well defined cooling regime transition indicating that it may lie outside of the transport current range investigated (approaching the critical current of 6000 to 7000 A for the 11T to 13T range). The results of the simulation do agree with experiment in that the stability curves are fairly flat, and thus show no transition in cooling regime.

References

- 1 Bottura L., “Limiting Current and Stability of Cable-in-conduit Conductors”, pg. 787, *Cryogenics* 34 (1994)
- 2 Koizumi N., Takahashi Y., Tsuji H., “Numerical Model Using an Implicit Finite Difference Algorithm for Stability Simulation of a Cable-in-conduit Superconductor”, *Cryogenics* 36 (1996)
- 3 Koizumi N., Takahashi Y., Tsuji H., et al., “Stability and Limiting Current of Cable-in-Conduit Superconductor for Short Length Perturbation”, JAERI internal publication
- 4 Carslaw H., Jaeger J., *Conduction of Heat in Solids*, Clarendon Press, Oxford, UK (1950)
- 5 Agatsuma A., “Influence of Mass Flow Rate and Hydraulic Perimeter in the Transient Stability Margin of a Forced Flow Cooled Superconductor”, pg. 551, *Cryogenics* 31 (1991)
- 6 Mills A. F., *Heat and Mass Transfer*, Richard D. Irwin, Inc. (1995)
- 7 Thompson F., Mastin C., “Boundary-fitted curvilinear coordinate systems for solution of partial differential equations on fields containing any number of arbitrary two-dimensional bodies”, NASA CR-2729 (1976)
- 8 Ito T., Tsuji H., et al, “Evaluation of Inductive Heating Energy of Sub-size Improved DPC-U Conductor by Calorimetric Method”, JAERI internal publication (1996)
- 9 Iwasa Y., *Case Studies in Superconducting Magnets*, Plenum Press, NY (1994)

Appendix - Code for POCHI v4 Implementation

```

SUBROUTINE KMTWS ( TWNI , TWCNI , TEMP , QTOTAL, QGIVEN,
1  QLOSS , QJOULE, QSS , QJSS , RCU , RSS ,
2  AIT , AID , TWNM1 , TWBNI , TWCNM1, TWCBNI,
3  AIDB , TCS , TC , GAMMST, GAMMAS, GAMMAC,
4  GAMMSS, RKC , RKSS , RAMDAC, RAMDSS, DRCDX ,
5  DRSSDX, THCOND, THCSS , GQCNST, XS , XS2 ,
6  RKHE , DEL , DELM1 , QFLUX , QFLSS , PLANDT,
7  HRAMDA, SPCFHT, REINOR, PDEFEC, HSFLAG, YNORM ,
8  YNS , YNS2 , YNODE , YS , YNODEM, TWHE ,
9  TWCHE , TWHEM1, TWCHM1, TWHEB , TWCHEB, ATWHE0,
A  ATWHE1, ATWHE2 )
C
C  IMPLICIT REAL*8 (A-H,O-Z)
C
C  SOLUTION OF HEAT CONDUCTION EQUATION ON TRANSFERED COORDINATE
C
C  INCLUDE 'INPUTC.inc'
C  INCLUDE 'COEFFC.inc'
C  INCLUDE 'CONSTC.inc'
C
C  DIMENSION TWNI (NI), TWCNI (NI), TEMP (NI), QTOTAL(NI),
1  QGIVEN(NI), QLOSS (NI), QJOULE(NI), QSS (NI),
2  QJSS (NI), RCU (NI), RSS (NI), AIT (NT),
3  AID (NI), TWNM1 (NI), TWBNI (NI), TWCNM1(NI),
4  TWCBNI(NI), AIDB (NI), TCS (NI), TC (NI),
5  GAMMST(NI), GAMMAS(NI), GAMMAC(NI), GAMMSS(NI),
6  RKC (NI), RKSS (NI), RAMDAC(NI), RAMDSS(NI),
7  DRCDX (NI), DRSSDX(NI), THCOND(NI), THCSS (NI),
8  GQCNST(NI), XS (NI), XS2 (NI), RKHE (NI),
9  DEL (NI), DELM1 (NI), QFLUX (NI), QFLSS (NI),
A  PLANDT(NI), HRAMDA(NI), SPCFHT(NI), REINOR(NI),
B  PDEFEC(NI), HSFLAG(NI),
C  YNORM (NY), YNS (NY), YNS2 (NY),
D  YNODE (NI,NY), YNODEM(NI,NY), YS (NI,NY),
E  TWHE (NI,NY), TWCHE (NI,NY), TWHEM1(NI,NY),
F  TWCHM1(NI,NY), TWHEB (NI,NY), TWCHEB(NI,NY),
G  ATWHE0(NI,NY), ATWHE1(NI,NY), ATWHE2(NI,NY)
C
C  #####
C  #          SETTING PARAMETERS          #
C  #####
C  ACU=area of copper in strand, AST=total strand area,ASU=area of superconducting
C  material,AEL=non copper or superconducting area,DHW=hydraulic diameter

```

```

ETACUW=ACU/AST
ETASUW=ASU/AST
ETAELW=AEL/AST
EPS1 =DELTAT*EPSTCE
DHW2 =DHW/2.0D0
C
C #####
C #          CALCULATION OF STRAND PROPERTIES          #
C #####
C GAMMST=effective volumetric heat capacity of the strand
C RAMDAC=thermal conductivity
  DO 4000 I=1,NI
    GAMMST(I)=(ETACUW+ETAELW)*GAMMAC(I)+ETASUW*GAMMAS(I)
    RKC(I)=ETACUW*RAMDAC(I)/GAMMST(I)
4000 CONTINUE
  DO 4010 I=2,NI-1
C DRCDX= $\Delta\lambda/\Delta x$ 
  DRCDX(I)=(RAMDAC(I+1)-RAMDAC(I-1))/(2.D0*DELTAX)
4010 CONTINUE
C
C #####
C #  CALCULATION OF CONDUIT PROPERTIES AND HEATING POWER  #
C #####
C RKSS same as RKC but for stainless steel in conduit
  DO 4100 I=1,NI
    RKSS(I)=RAMDSS(I)/GAMMSS(I)
4100 CONTINUE
  DO 4110 I=2,NI-1
C DRSSDX same as DRCDX but for conduit
  DRSSDX(I)=(RAMDSS(I+1)-RAMDSS(I-1))/(2.D0*DELTAX)
4110 CONTINUE
C
C #####
C #          CALCULATION OF KAPPITZ CONDUCTANCE          #
C #####
C
  IF( ITIME.EQ.2) THEN
    DO 4200 I=1,NI
      THCOND(I)=8.0D2*TWNI(I)**3
      THCSS(I)=8.0D2*TWCNI(I)**3
4200 CONTINUE
C
  ELSE
    DO 4210 I=1,NI
C This is heat transfer coefficient as per equation 4
    IF(TWNI(I).NE.TWHE(I,1)) THEN

```



```

      THCOND(I)=2.0D2*(TWN(I)**4-TWHE(I,1)**4)
1      /(TWN(I)-TWHE(I,1))
      ELSE
      THCOND(I)=8.0D2*TWN(I)**3
      ENDIF
C
      IF(TWCNI(I).NE.TWCHE(I,1)) THEN
      THCSS(I)=2.0D2*(TWCNI(I)**4-TWCHE(I,1)**4)
1      /(TWCNI(I)-TWCHE(I,1))
      ELSE
      THCSS(I)=8.0D2*TWCNI(I)**3
      ENDIF
4210 CONTINUE
      ENDIF
C
C #####
C #      CALCULATION OF BOUNDARY LAYER THICKNESS      #
C #####
C
DO 4300 I = 1,NI
C
C      Laminar Flow Heat Transfer Coefficient
C
      HSL=4.0D0*HRAMDA(I)/DHW
C
C      Turbulent Flow Heat Transfer Coefficient
C      Variation of equation 7 for turbulent case used by Koizumi
      IF(NHTSSL.EQ.0) THEN
      HST=2.3D-2*HRAMDA(I)*REINOR(I)**0.8D0*PLANDT(I)**0.4D0/DHW
      ELSE IF(NHTSSL.EQ.1) THEN
      HST=PDEFEC(I)/8.0D0*HRAMDA(I)*REINOR(I)*PLANDT(I)**0.4D0/DHW
      ELSE
      HST=2.6D-2*HRAMDA(I)*REINOR(I)**0.8D0*PLANDT(I)**0.4D0/DHW
      & *(TEMP(I)/TWN(I)**0.716D0
      END IF
C
C      Setting Steady Heat Transfer Coefficient
C
      IF(HSL.GE.HST) THEN
      HS=HSL
      HSFLAG(I)=0.1D0
      DEL(I)=DHW2
      ELSE
      HS=HST
      HSFLAG(I)=1.1D0
      DEL(I) = HRAMDA(I)/HS

```

```

        IF(DEL(I).GT.DHW2) THEN
            DEL(I)=DHW2
        ENDIF
    END IF
C
C    Boundary layer thickness
C
    DO 4310 IY = 1,NY
        YNODEM(I,IY) = YNODE(I,IY)
4310 CONTINUE
C #####
C #          Y-COORDINATE TRANSFER          #
C #####
C Implementation of coordinate transfer as per Thompson and Mastin
    RKHE(I)= HRAMDA(I)/SPCFHT(I)
    YABFC0 = 2.0D1*DEL(I)*SQRT(PI*FREQ)*DELTAY/SQRT(RKHE(I))
    YABFC = YABFC0-1.0D0
    YCBFC = 7.0D-1*DEL(I)/YABFC0
C
    CALL KMCAT( YNORM , YNS , YNS2 , DEL, YABFC, YCBFC, I)
C
    YNODE(I,1) = YNORM(1)
    YS(I,1) = YNS(1)
    DO 4320 IY = 2,NY-1
        YNODE(I,IY) = YNORM(IY)
        YS(I,IY) = YNS(IY)
        ATC0=RKHE(I)*DELTAT/(YS(I,IY)**2*DY2)
        ATWHE0(I,IY)=1.0D0+2.0D0*ATC0
        ATC1=YNS2(IY)*DELTAY/(2.0D0*YS(I,IY))
        ATWHE1(I,IY)=(1.0D0+ATC1)*ATC0
        ATWHE2(I,IY)=(1.0D0-ATC1)*ATC0
4320 CONTINUE
        YNODE(I,NY) = YNORM(NY)
        YS(I,NY) = YNS(NY)
4300 CONTINUE
C
C #####
C #    CALCULATION OF TWHE, TWCHE AT PREVIOUS TIME STEP    #
C #####
    DO 4330 I=1,NI
        NY1=2
        TWHEM1(I,1)=TWHE(I,1)
        TWCHM1(I,1)=TWCHE(I,1)
        DO 4340 IY=2,NY-1
            IF(YNODE(I,IY).GE.DELM1(I)) THEN
                TWHEM1(I,IY)=TWHE(I,NY)

```

```

    TWCHM1(I,IY)=TWCHE(I,NY)
ELSE
DO 4350 IY1=NY1,NY
    IF (YNODEM(I,IY1).GT.YNODE(I,IY)) THEN
        NY1=IY1
C
        GO TO 3000
C
        ENDIF
4350 CONTINUE
3000 TWHEM1(I,IY)=( YNODEM(I,NY1)-YNODE(I,IY))
    1 *TWHE(I,NY1-1)
    2 +(YNODE(I,IY)-YNODEM(I,NY1-1))*TWHE(I,NY1) )
    3 / (YNODEM(I,NY1)-YNODEM(I,NY1-1))
    TWCHM1(I,IY)=( YNODEM(I,NY1)-YNODE(I,IY))
    1 *TWCHE(I,NY1-1)
    2 +(YNODE(I,IY)-YNODEM(I,NY1-1))*TWCHE(I,NY1) )
    3 / (YNODEM(I,NY1)-YNODEM(I,NY1-1))
    ENDIF
4340 CONTINUE
    TWHEM1(I,NY)=TWHE(I,NY)
    TWCHM1(I,NY)=TWCHE(I,NY)
4330 CONTINUE
C
DO 4360 I=1,NI
    DO 4370 IY=1,NY
        TWHE(I,IY)=TWHEM1(I,IY)
        TWCHE(I,IY)=TWCHM1(I,IY)
4370 CONTINUE
4360 CONTINUE
C
    NTCE=0
3100 NTCE=NTCE+1
    EPSMAX=0.D0
    DO 4400 I=1,NI
        TWBNI(I)=TWNI(I)
        TWCBNI(I)=TWCNI(I)
        AIDB(I)=AID(I)
        DO 4410 IY=1,NY
            TWHEB(I,IY) =TWHE(I,IY)
            TWCHEB(I,IY)=TWCHE(I,IY)
4410 CONTINUE
4400 CONTINUE
C
C #####
C # SOLVING INDUCED CURRENT EQ BETWEEN STRANDS AND CONDUIT #

```

```

C #####
C
IF(G.GT.0.0D0) THEN
C
  IF(AIT(ITIME).EQ.0.0D0) THEN
    DO 4500 I=1,NI
      AID(I)=0.0D0
      GQCNST(I)=0.0D0
4500  CONTINUE
    ELSE
      AID(1)=0.0D0
      DO 4510 I=2,NI-1
        IF(TWNI(I).LT.TCS(I)) THEN
          GQCNST(I)=0.0D0
        ELSE IF(TWNI(I).GE.TC(I)) THEN
          GQCNST(I)=1.0D0
        ELSE
          GQCNST(I)=( TWNI(I)-TCS(I) ) / ( TC(I)-TCS(I) )
        END IF
        RST=RCU(I)*GQCNST(I)/ACU
        COEFB=GDX2*(RST+RSS(I)/ASS)
        COEFW=OMEGA/(2.0D0+GDX2*(RST+RSS(I)/ASS)*XS(I)**2)
        AID(I)=(1.0D0-OMEGA)*AID(I)
1          +COEFW*( AID(I-1)+AID(I+1)
2          -XS2(I)*DELTA*(AID(I+1)-AID(I-1))/(2.0D0*XS(I))
3          +GDX2*RST*XS(I)**2*AIT(ITIME))
4510  CONTINUE
        AID(NI)=0.0D0
        DO 4520 I=2,NI-1
          ADEPS=ABS((AID(I)-AIDB(I))/AIT(ITIME))
          IF(ADEPS.GE.EPSMAX) THEN
            EPSMAX=ADEPS
          END IF
4520  CONTINUE
        END IF
C
      ELSE
C
        DO 4530 I=1,NI
          AID(I)=0.0D0
4530  CONTINUE
        DO 4540 I=2,NI-1
          IF(TWNI(I).LT.TCS(I)) THEN
            GQCNST(I)=0.0D0
          ELSE IF(TWNI(I).GE.TC(I)) THEN
            GQCNST(I)=1.0D0

```

```

ELSE
  GQCNST(I)=(TWN1(I)-TCS(I))/(TC(I)-TCS(I))
END IF
4540 CONTINUE
C
END IF
C
C #####
C #      CALCULATION OF JOULE HEATING POWER          #
C #####
C
CALL CALQJL(QJOULE, QJSS , RCU , RSS , AIT , AID )
C
C #####
C #      CALCULATION OF TOTAL HEATING POWER INTO STRANDS  #
C #####
C
DO 4600 I=1,NI
  QTOTAL(I)=QGIVEN(I)+QLOSS(I)+GQCNST(I)*QJOULE(I)
4600 CONTINUE
C
C #####
C #      SOLVING THERMAL CONDUCTIVITY EQUATION FOR STRANDS  #
C #####
C This section of the routine contains the differences between POCHI v3 and v4.
C TWNI is the x direction mesh for the temperature in the strand
C TWHE is the array holding values for the helium temperature mesh
C Loop 4700 remains essentially unchanged except for the redefinition of  $q_{st}$  in
C equation 2 in terms of Kappitza conductance THCOND and the first node in the
C coolant mesh TWHE.
  TWNI(1)=(1.D0-BOMEGA)*TWNI(1)
  1  +BOMEGA/3.D0*(4.D0*TWNI(2)-TWNI(3))
  DO 4700 I=2,NI-1
    COEFW=OMEGA/(1.D0+2.D0*RKC(I)/(DX2DT*XS(I)**2)
  1  +(THCOND(I)*PERI+THSTSS*PERISS)*DELTAT
  2  /(AST*GAMMST(I))
    TWNI(I)=(1.D0-OMEGA)*TWNI(I)
  1  +COEFW*(RKC(I)/(DX2DT*XS(I)**2)*(TWNI(I+1)+TWNI(I-1))
  2  -(RAMDAC(I)*XS2(I)/XS(I)-DRCDX(I))*ETACUW
  3  /(GAMMST(I)*XS(I))*DELTAT/XS(I)
  4  *(TWNI(I+1)-TWNI(I-1))/(2.D0*DELTA X)
  5  +TWNM1(I)
  6  +(THCOND(I)*PERI*TWHE(I,1)+THSTSS*PERISS*TWCNI(I))
  7  *DELTAT/(AST*GAMMST(I))
  8  +DELTAT/GAMMST(I)*QTOTAL(I)
4700 CONTINUE

```

```

      TWNI(NI) = (1.D0-BOMEGA)*TWNI(NI)
1      + BOMEGA/3.D0*(4.D0*TWNI(NI-1)-TWNI(NI-2))
C
C After the iteration of strand temperatures is completed then the coolant temperature
C mesh is solved for in the nested loops of 4710 and 4720. I is the x direction counter and
C IY the y direction counter.
C YS=yξ, DELTAY=Δξ
      DO 4710 I=1,NI
          COEFYB =HRAMDA(I)/(2.0D0*YS(I,1)*DELTAY)
C Set the first boundary condition at the strand surface as per equation 3b
          TWHE(I,1)=(1.0D0-BOMEGA)*TWHE(I,1)+BOMEGA
1          /(THCOND(I)+3.0D0*COEFYB)
2          *(THCOND(I)*TWNI(I)+COEFYB*(4.0D0*TWHE(I,2)-TWHE(I,3)))
          DO 4720 IY = 2,NI-1
C The equation below is equation 10 where ATWHE1 and ATWHE2 are common terms
C in equation 10 calculated in an earlier routine to make calculation here simpler
          TWHE(I,IY)= (1.D0-OMEGA)*TWHE(I,IY)+OMEGA/ATWHE0(I,IY)
1          *( ATWHE1(I,IY)*TWHE(I,IY-1)
2          + ATWHE2(I,IY)*TWHE(I,IY+1)+TWHEM1(I,IY) )
4720 CONTINUE
C Set second boundary condition as per equation 3a
          IF(INT(HSFLAG(I)).EQ.0) THEN
              TWHE(I,NI)=BOMEGA*TWHE(I,NI)
1              +(1.0D0-BOMEGA)*(4.0D0*TWHE(I,NI-1)-TWHE(I,NI-2))/3.0D0
          ELSE
              TWHE(I,NI)=TEMP(I)
          ENDIF
4730 CONTINUE
4710 CONTINUE
C
      DO 4740 I=1,NI
          TWEPS=ABS((TWNI(I)-TWBNI(I))/TWNI(I))
          IF( TWEPS .GE. EPSMAX ) THEN
              EPSMAX=TWEPS
          END IF
          DO 4750 IY=1,NI
              TWEPS=ABS((TWHE(I,IY)-TWHEB(I,IY))/TWHE(I,IY))
              IF(TWEPS .GE. EPSMAX) THEN
                  EPSMAX=TWEPS
              END IF
          4750 CONTINUE
          4740 CONTINUE
C
C #####
C # CALCULATION OF TOTAL HEATING POWER INTO CONDUIT #
C #####

```

```

C
DO 4800 I=1,NI
  TWHE(I,NY)=TEMP(I)
  ENDIF
4730 CONTINUE
4710 CONTINUE
C
DO 4740 I=1,NI
  TWEPS=ABS((TWN(I)-TWBNI(I))/TWN(I))
  IF( TWEPS .GE. EPSMAX ) THEN
    EPSMAX=TWEPS
  END IF
DO 4750 IY=1,NY
  TWEPS=ABS((TWHE(I,IY)-TWHEB(I,IY))/TWHE(I,IY))
  IF(TWEPS .GE. EPSMAX) THEN
    EPSMAX=TWEPS
  END IF
4750 CONTINUE
4740 CONTINUE
C
C #####
C #   CALCULATION OF TOTAL HEATING POWER INTO CONDUIT   #
C #####
C
DO 4800 I=1,NI
  QSS(I)=YETAH*QGIVEN(I)+QJSS(I)
4800 CONTINUE
C
C #####
C #   SOLVING THERMAL CONDUCTIVITY EQUATION FOR CONDUIT   #
C #####
C As noted earlier heat conduction from the conduit remains the same as for POCHI v3 and
C remains unchanged here from the earlier version
TWCNI(1)=(1.D0-BOMEGA)*TWCNI(1)
1   +BOMEGA/3.D0*(4.D0*TWCNI(2)-TWCNI(3))
DO 4900 I=2,NI-1
  COEFW=OMEGA/(1.D0+2.D0*RKSS(I)/(DX2DT*XS(I)**2)
1   +(THCSS(I)+THSTSS)*PERISS*DELTAT/(ASS*GAMMSS(I)))
  TWCNI(I)=(1.D0-OMEGA)*TWCNI(I)
1   +COEFW*( RKSS(I)/(DX2DT*XS(I)**2)
2   *(TWCNI(I+1)+TWCNI(I-1))
3   -(RAMDSS(I)*XS2(I)/XS(I)-DRSSDX(I))
4   /(GAMMSS(I)*XS(I))*DELTAT/XS(I)
5   *(TWCNI(I+1)-TWCNI(I-1))/(2.D0*DELTAX)
6   +TWCNM1(I)
7   +(THCSS(I)*TWCHE(I,1)+THSTSS*TWN(I))*PERISS*DELTAT

```

```

8      /(ASS*GAMMSS(I))
9      +DELTAT/GAMMSS(I)*QSS(I)
4900 CONTINUE
      TWCNI(NI)=(1.D0-BOMEGA)*TWCNI(NI)
1      +BOMEGA/3.D0*(4.D0*TWCNI(NI-1)-TWCNI(NI-2))
C
DO 4910 I=1,NI
      COEFYB =HRAMDA(I)/(2.0D0*YS(I,1)*DELTAY)
      TWCHE(I,1)=(1.0D0-BOMEGA)*TWCHE(I,1)+BOMEGA
1      /(THCSS(I)+3.0D0*COEFYB)
2      *(THCSS(I)*TWCNI(I)
3      +COEFYB*(4.0D0*TWCHE(I,2)-TWCHE(I,3)))
DO 4920 IY = 2,NY-1
      TWCHE(I,IY)= (1.D0-OMEGA)*TWCHE(I,IY)+OMEGA/ATWHE0(I,IY)
1      *( ATWHE1(I,IY)*TWCHE(I,IY-1)
2      + ATWHE2(I,IY)*TWCHE(I,IY+1)+TWCHM1(I,IY) )
4920 CONTINUE
      IF(INT(HSFLAG(I)).EQ.0) THEN
          TWCHE(I,NY)=BOMEGA*TWCHE(I,NY)
1          +(1.0D0-BOMEGA)*(4.0D0*TWCHE(I,NY-1)-TWCHE(I,NY-2))
2          /3.0D0
      ELSE
          TWCHE(I,NY)=TEMP(I)
      ENDIF
4910 CONTINUE
C
DO 4940 I=1,NI
      TWCEPS=ABS((TWCNI(I)-TWCBN(I))/TWCNI(I))
      IF(TWCEPS.GE.EPSMAX) THEN
          EPSMAX=TWCEPS
      END IF
      DO 4950 IY=1,NY
          TWCEPS=ABS((TWCHE(I,IY)-TWCHEB(I,IY))/TWCHE(I,IY))
          IF(TWCEPS .GE. EPSMAX) THEN
              EPSMAX=TWCEPS
          END IF
4950 CONTINUE
4940 CONTINUE
C
      IF( EPSMAX .GT. EPS1 ) GO TO 3100
C
DO 5000 I=1,NI
      QFLUX(I)=THCOND(I)*(TWCNI(I)-TWHE(I,1))
      QFLSS(I)=THCSS(I)*(TWCNI(I)-TWCHE(I,1))
5000 CONTINUE
C

```



```
DO 5100 I=1,NI
  IF(INT(HSFLAG(I)).EQ.(NY-1)/2) THEN
    DELM1(I)=DEL(I)
  ELSE
    DELM1(I)=DHW2
  ENDIF
5100 CONTINUE
C
  RETURN
END
```